Effects of polarized organosilane self-assembled monolayers on organic single-crystal field-effect transistors

J. Takeya[1,*],* T. Nishikawa[2,3,5], T. Takenobu[2,4], S. Kobayashi[2,4], C. Goldmann[6], C. Krellner[6], T. Shimoda[3,5], T. Mitani[5], Y. Iwasa[2,4], and B. Batlogg[6]
[1]*Materials Science Research Laboratory, CRIEPI, Tokyo 201-8511, Japan*
[2]*Institute for Material Reasearch, Tohoku University, Sendai 980-8577, Japan*
[3]*Technology Platform Research Center, SEIKO EPSON Corporation, Fujimi, Nagano 399-0293, Japan*
[4]*CREST, Japan Science and Technology Corporation, Kawaguchi 333-0012, Japan*
[5]*Japan Advanced Institute of Science and Technology, Tatsunokuchi, Ishikawa 923-1292, Japan and*
[6]*Laboratory for Solid State Physics ETH, CH-8093 Zürich, Switzerland*
(Dated: February 2, 2008)

The surface conductivity is measured by a four-probe technique for pentacene and rubrene single-crystals laminated on polarized and nearly unpolarized molecular monolayers with application of perpendicular electric fields. The polarization of the self-assembled monolayers (SAMs) shifts the threshold gate voltage, while maintaining a very low subthreshold swing of the single-crystal devices (0.11 V/decade). The results, excluding influences of parasitic contacts and grain boundaries, demonstrate SAM-induced nanoscale charge injection up to $\sim 10^{12}$ cm^{-2} at the surface of the organic single crystals.

PACS numbers:

Significant efforts are being made to bring organic field-effect transistors (OFETs) into practical use, taking advantages of their potential of low-cost production, mechanical flexibility and optical as well as chemical sensitivities [1]. To promote the development, some basic questions are to be further elucidated, such as the intrinsic nature of the transport of charge induced at the surface of the organic semiconductors. Following this direction, a growing number of experiments has recently been reported on the single-crystal devices that avoid complication due to grain boundaries [2, 3, 4, 5, 6, 7]. In an early study of the single-crystal OFETs, Takeya *et al.* proposed a method of laminating organic crystals on SiO_2/doped Si substrates by natural electrostatic force [3]. Four-probe measurements on the single-crystal devices revealed genuine transfer characteristics of the OFETs, free from parasitic contact effects. In addition, the laminated single-crystal devices are also useful to examine whether a new finding in polycrystalline thin-film OFETs is intrinsic to the semiconductor-SiO_2 interface or is an artifact due to grain-boundaries, because the process of single-crystal device fabrication is identical to the commonly studied bottom-electrode thin-film OFETs. Note that inter-grain charge dynamics dominates the field-effect properties in some thin-film devices [8]

Self-assembled monolayers (SAMs) of neutral organosilane molecules are often incorporated in thin-film OFETs to passivate the SiO_2 surface before evaporating the organic semiconductor [9]. Very recently, Kobayashi *et al.* reported that the threshold gate voltage V_{th} is shifted in their polycrystalline thin-film devices when the neutral SAMs are replaced with highly electron-affine ones [10]. The mechanism of the threshold shift ΔV_{th}, however, was not clear; rather large standard deviation among the samples causes difficulty in quantitative comparison of ΔV_{th} among different thin-film materials and to the calculated dipole moment of the SAMs. Since the inclusion of grain boundaries and contact resistances may introduce complications [11], single-crystal samples are more appropriate to further study the microscopic mechanism of the observed shift. In the present work, we laminated pentacene and rubrene crystals on both polarized and on nearly unpolarized SAMs, to measure the field-effect conductivity using the four-terminal method. We reproduce the clear difference in V_{th} between the devices with the two different types of the SAMs, which demonstrates that charge is indeed induced at the surface of the crystal by the adjacent polarized organosilane molecules. The amount of the doped surface charge, however, significantly differs between the two organic materials, which cannot be explained by simple electronic response to the polarized substrates.

The single-crystal devices are prepared similarly to the processes described in 3. In an additional step, before placing the crystals onto the substrates, we carefully deposited decyltriethoxysilane or perfluorotriethoxysilane onto the SiO_2 gate dielectric by chemical vapor deposition (CVD) technique at 150°C to form neutral CH_3-terminated SAMs (CH_3-SAMs) or electron-affine F-terminated SAMs (F-SAMs), respectively. Typical channel dimensions are a length of around 7 μm and a width of 40 μm. We used the circuitry established in Ref. 3 for the four-terminal measurements employing four source-measure units (SMUs) of an Agilent Technology E5207 semiconductor parameter analyzer [Inset Fig. 1(a)]. Since we are interested in the on-off switching, particular attention is paid to reliable determination of

*Electronic address: takeya@criepi.denken.or.jp

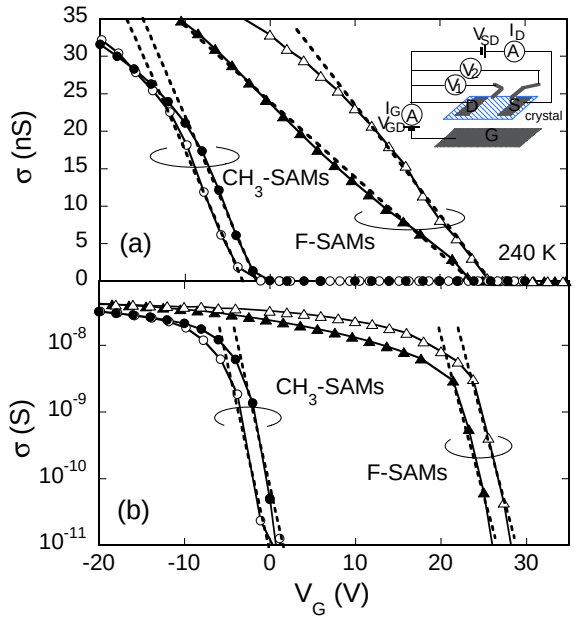

FIG. 1: Main panel: Four-probe conductivity vs. gate voltage of pentacene single-crystal FETs with CH_3-SAMs and F-SAMs at 240 K; (a) a linear plot and (b) a logarithmic plot. Inset: The circuit diagram of the four-terminal measurement. The dashed lines are drawn to estimate μ in (a) and S in (b).

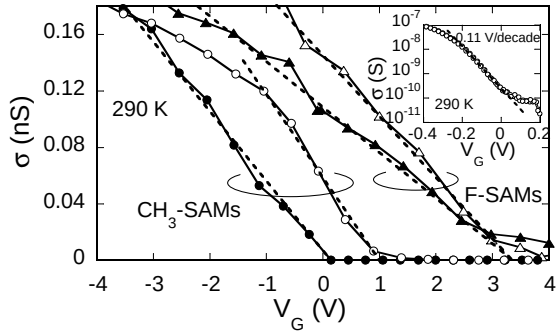

FIG. 2: Four-probe conductivity vs. gate voltage for rubrene single-crystal FETs. Main panel: comparison between CH_3-SAMs samples and F-SAMs samples at 290 K. The thickness of the SiO_2 is $\sim$ 500 nm. The inset shows results for a CH_3-SAM sample with a SiO_2 layer of less than 100 nm thickness. The dashed lines were used to estimate μ in the main panel and S in the inset.

V_{th}. We set V_D to be small enough so that the $I-V$ characteristics of the channel remain ohmic; otherwise, V_{th} would move to the positive-V_G direction in the non-ohmic regime (when the carriers are holes).

In the main panel of Fig. 1(a), we plot the transfer characteristics of two CH_3-SAM samples and two F-SAM samples. The horizontal axis represents the gate voltage V_G applied to the central part in the channel, which is given by $V_G = V_{GS} + (V_1 + V_2)/2$. Hysteresis is negligible at 240 K when the gate voltage is swept back and forth in helium atmosphere. Though pronounced hysteresis appears at room temperature, introducing some ambiguity in the determination of V_{th}, the hysteresis quickly diminishes with decreasing temperature. The threshold voltage, however, remained essentially unchanged between 240 K and 290 K.

TABLE I: Device parameters of the measured single-crystal FETs. d_i, μ, V_{th}, S, D_{it} represent thickness of SiO_2 dielectrics, mobility, threshold voltage, subthreshold swing, and interface-trap density, respectively.

Material	SAMs	d_i (μm)	μ (cm^2/Vs)	V_{th} (V)	S (V/decade)	D_{it} (10^{11} /cm^2eV)
pentacene	CH_3-	~ 0.5	~ 0.4	~ -3.5	~ 1.5	~ 9
pentacene	CH_3-	~ 0.5	~ 0.4	~ -1.5	~ 1.5	~ 9
pentacene	F-	~ 0.5	~ 0.15	~ 24	~ 2	~ 20
pentacene	F-	~ 0.5	~ 0.2	~ 26	~ 2	~ 20
rubrene	CH_3-	~ 0.5	~ 7	~ 0	~ 0.4	~ 2
rubrene	CH_3-	~ 0.5	~ 8	~ 0.8	~ 0.7	~ 4
rubrene	F-	~ 0.5	~ 4	~ 3.5	~ 0.9	~ 5
rubrene	F-	~ 0.5	~ 5	~ 3.5	~ 1.3	~ 7
rubrene	CH_3-	< 0.1	~ 6	~ -0.1	~ 0.11	~ 2

Fundamental parameters of the samples are listed in Table 1. Obviously V_{th} differs among the two groups of pentacene single-crystal FETs; the two CH_3-SAM samples switch on at around 0 V, while the two F-SAM samples do around 25 V. The corresponding difference in the gate threshold field E_{th} is estimated to be $\sim$ 0.5 MV/cm, which is comparable to the value $\sim$ 0.7-1 MV/cm reported for polycrystalline thin-film pentacene FETs [10, 11]. Noting that the present four-terminal measurements on the single crystals are free from complications such as grain boundaries and parasitic contact effects, the threshold voltage shift is an intrinsic effect at the interface between the well-ordered SAM molecules and the almost perfectly ordered pentacene molecules.

The interface quality manifests itself in sharp on-off switching as illustrated in Fig. 1(b) on a logarithmic scale. The subthreshold swing S of the pentacene devices are around 2 V/decade. This value indicates that the interface trap density is at least comparable to or better than that of the best pentacene thin-film FETs as compared with literatures [12, 13], taking into account the rather thick dielectric layer in the present devices (SC_i is evaluated $\sim$ 14 nVF/decade cm^2 as renormalized by the capacitance C_i of the gate dielectrics per area).

In order to examine the universality of the above observation, we have also measured the four-probe surface conductivity of rubrene single-crystal FETs, prepared in exactly the same way as the pentacene devices. Figure 2 shows the transfer characteristics of the rubrene devices with CH_3-SAMs or F-SAMs, which were deposited under the same conditions as for the pentacene devices. The mobilities estimated from the slopes in the on-state are listed in Table 1 together with other device parameters. The values are comparable to former reports on both similarly prepared rubrene single-crystal field-effect devices and devices with softly deposited polymeric gate insulators [2, 5, 14]. Because of negligible hysteresis of our rubrene FETs, the comparison of V_{th} is only made

at room temperature this time.

The threshold voltage of the rubrene devices shift with the intrinsic polarization of the SAMs as it did for the pentacene samples; however, the difference in V_{th} is only around 3.5 V, which is much smaller than $\sim$ 25 V for the pentacene devices. Since we have excluded artifacts from grain boundaries and contacts to the electrodes, it is natural to consider that the electron affinity of the F-SAMs indeed induces charge redistribution at the surface of the pentacene and rubrene crystals. To remove the excess holes, the gate electric field $E_{th} = V_{th}/d_i$, where d_i is thickness of the gate insulator, is needed; in other words, the density of excess holes induced by the F-SAMs is $p_0 = \epsilon\epsilon_0 E_{th}$, where $\epsilon\epsilon_0$ is the dielectric permittivity of the gate insulator. Taking the values of V_{th} for the pentacene and rubrene devices, the excess hole density is estimated to be $p_0 \sim 1.1 \times 10^{12}$ cm^{-2} and $\sim 1.5 \times 10^{11}$ cm^{-2}, respectively, assuming $\epsilon \sim 3.9$ for the thermally oxidized SiO_2.

Sugimura *et al.* reported that surface potential differs by $\sim$ 0.2 V between the F-SAMs and the CH_3-SAMs deposited on SiO_2 based on their Kelvin-probe measurement [15]. On the other hand, the dipole moment of free-standing F-SAMs μ, which is calculated to be $\sim$ 2 Debye, would give the potential difference ΔV_s of 0.4-1.1 V (depending on assumed SAM density N) as $\Delta V_s = N\mu/\epsilon_{SAM}\epsilon_0$ [10]. Note that the latter can overestimate ΔV_s because it neglects any depolarization effects as the molecules form the layer. Taking the smallest value $\sim$ 0.2 V of ΔV_s, still a gate potential as high as $\sim$ 100 V across our gate dielectric is necessary to compensate the surface potential induced by the 1-nm thick F-SAMs. As compared to our experimental results, ΔV_{th} is significantly smaller than the above estimation, indicating presence of other depolarization mechanism(s) involving the organic crystals. Moreover, the observation that p_0 significantly differs between the pentacene and rubrene devices supports the idea of the charge rearrangement *in* the crystals. Microscopically, ionic relaxation in response to the local electric field [16, 17] may be a possible cause of the redistribution of the (acceptor-type) interface-trap states [18, 19]. Further theoretical and experimental studies are necessary to fully elucidate this mechanism of SAM-induced surface charge doping.

Finally, the subthreshold swing S of the rubrene devices shall be discussed. For the four devices shown in Fig. 2, S is evaluated to be 0.4-1.3 V/decade, which is smaller than the values for the pentacene devices (listed in Table 1). We have also measured another rubrene device attached on thinner (< 100 nm) SiO_2, coated with a CH_3-SAM. The inset to Fig. 2 shows the transfer characteristics of this device. The slope of 0.11 V/decade measured in this device is the smallest value reported so far for organic FETs and is comparable to the value of the best inorganic devices 0.07 V/decade. This is the result of the high-quality interface of the rubrene-single crystal devices. A well-known simple equation relates S to density of shallow trap levels (within the thermal energy), $S = k_B T/eln(10)(1 + C_{it}/C_i)$, where C_{it} is the capacitance due to the interface traps [k_B is the Boltzmann constant and e is the electric charge]. The interface-trap density D_{it} is simply given by C_{it}/e [20]. Because of thermal diffusion, the steepness is limited by the first term in parentheses of the right-hand side of the equation. As we list in Table 1, D_{it} for the rubrene devices is roughly one order smaller than that of the pentacene devices. This estimation, derived from a four-probe measurement, gives an intrinsic shallow-trap density excluding artifacts from the contacts. The difference in S between the pentacene and rubrene devices indicates that the interface traps are located inside the organic materials rather than in SiO_2. For pentacene, the estimation is consistent with an independent evaluation by optical measurement [19].

In summary, the incorporation of self-assembled monolayers provides a variety of new possibilities for FETs of laminated single crystals. The highly ordered interface between the self-aligned silane molecules and the surface of the molecular crystal facilitates an outstanding field-effect response, demonstrated for a rubrene device as the steepest subthreshold swing 0.11 V/decade ever reported. The use of polarized F-SAMs demonstrated that holes are accumulated as a result of nanometer scale charge rearrangement near the interface between the crystal and the gate oxide. From a technical aspect, the present results suggest that the switching gate voltages can be tuned by choosing the appropriate SAM molecule from a large number of available materials. Combined with the excellent subthreshold characteristics, this technique may prove useful for implementation in low-power applications such as logic components.

The authors acknowledge helpful discussions with D. J. Gundlach and technical support by S. Mori. This study was partially supported by a Grant-in-Aid for Scientific Research (No. 16740214) from the Ministry of Education, Culture, Sports, Science, and Technology, Japan. We also thank the Swiss National Science Foundation for financial support.

[1] C. Dimitrakopoulos and P. Malenfant, Adv. Mater. **14**, 99 (2002).
[2] V. Podzorov *et al.*, Appl. Phys. Lett. **82**, 1739 (2003).
[3] J. Takeya *et al.*, J. Appl. Phys. **94**, 5800 (2003).
[4] R. W. I. de Boer *et al.*, Appl. Phys. Lett. **83**, 4345 (2003).
[5] V. Podzorov *et al.*, Appl. Phys. Lett. **83**, 3504 (2003).
[6] T. Hasegawa *et al.*, Pys. Rev. B **69**, 245115 (2004).
[7] V. C. Sundar *et al.*, Science **83**, 4345 (2004).
[8] G. Horovitz *et al.*, J. Appl. Phys. **87**, 4456 (2000).
[9] D. J. Gundlach *et al.*, IEEE Electr. Dev. Lett. **22**, 571 (2001).
[10] S. Kobayashi *et al.*, Nature Mat. **3**, 317 (2004).

[11] K. P. Pernstich *et al.*, preprint (2004).
[12] D. J. Gundlach *et al.*, Appl. Phys. Lett. **80**, 2925 (2002).
[13] D. Knipp *et al.*, J. Appl. Phys. **93**, 347 (2003).
[14] C. Goldamann *et al.*, cond-mat/0403210 (2004).
[15] H. Sugimura *et al.*, Appl. Surf. Sci. **188**, 403 (2002).
[16] J. E. Northrup and M. L. Chabinye, Phys. Rev. B **68**, R041202 (2003).
[17] D. B. A. Rep *et al.*, J. Appl. Phys. **4**, 2082 (2003).
[18] A. R. Voelkel *et al.*, Phys. Rev. B **66**, 195336 (2002).
[19] D. V. Lang *et al.*, cond-mat/0312722 (2003).
[20] M. Pope and C. Swenberg, *Electronic Processes in Organic Crystals and Polymers, 2nd ed.* (Oxford University Press, 1999).